Measurement of Fibrin Concentration by Fast Field-Cycling NMR

Lionel M Broche[1*], Saadiya R Ismail[1, 2*,] Nuala A Booth[2] and David J Lurie[1]

[1] Aberdeen Biomedical Imaging Centre, School of Medical Sciences, University of Aberdeen, AB25 2ZD, UK.

[2] Institute of Medical Sciences, University of Aberdeen, AB25 2ZD, UK

Word Count: 2858

*Note that these first authors contributed equally to the paper.

Corresponding Author: David J. Lurie, email: d.lurie@abdn.ac.uk

Abstract

The relaxation of ^{1}H nuclei due to their interaction with quadrupolar ^{14}N nuclei in gel structures is measured using fast field-cycling (FFC) NMR. This phenomenon called quadrupolar dips has been reported in different ^{1}H-^{14}N bond-rich species. In this study we have studied quadrupolar dips in fibrin, an insoluble protein that is the core matrix of thrombi. Fibrin was formed by the addition of thrombin to fibrinogen in 0.2 % agarose gel. T_1-dispersion curves were measured using FFC NMR relaxometry, over the field range 1.5 - 3.5 MHz (proton Larmor frequency) and were analysed using a curve fitting algorithm. A linear increase of signal amplitude with increasing fibrin concentration was observed. This agrees with the current theory that predicts a linear relationship of signal amplitude with the concentration of contributing ^{14}N spins in the sample. Interestingly, fibrin formation gave rise to the signal, regardless of cross-linking induced by the transglutaminase factor XIIIa. In order to investigate the effect of proteins that might be trapped in the thrombi *in vivo*, the plasma protein albumin was added to the fibrin gel and an increase in the quadrupolar signal amplitude was observed. This study can potentially be useful for thrombi classification by FFC-MRI techniques.

Keywords: fast field-cycling, relaxometry, fibrin, quadrupolar dip

Introduction

The technique of fast field-cycling (FFC) which involves rapidly changing the magnetic field during a pulse sequence has developed steadily during the last three decades (1). The ability to investigate the behaviour of a sample over a range of magnetic strengths has proved useful to investigate molecular dynamics (2), in particular for the identification of quadrupole dips in a way that cannot be examined using fixed-field NMR (3). With the recent incorporation of FFC techniques into MRI, this technique opens up even more possibilities on living tissues and organic materials (4).

In this study we focus on the ^{1}H-^{14}N quadrupole dips previously observed in several experiments (5). Quadrupole dips and related phenomena have been previously measured using a number of methods and various types of sample, such as amino acids and nucleic bases (6), liquid crystalline material in the solid state (7) or monitoring of the concentration of immobilised protein (8). As the spin of the ^{14}N nucleus is 1, it possesses a quadrupolar moment that makes it relax very efficiently by coupling with the lattice. Magnetisation transfer from water protons to ^{14}N can happen at a short range and leads to an increase in water proton relaxation (9). This additional relaxation pathway occurs when one of the nuclear quadrupolar energy levels matches the ^{1}H Larmor frequency, generating dips in the T_1 dispersion curve called quadrupole dips at three distinct magnetic fields (or Larmor frequencies), typically 16 mT, 49 mT and 65 mT (9). However, this process can only happen when the NH bond is sufficiently immobilised compared to the coupling frequency, which means in practice that it is observed in gels, solids and liquid crystal samples, but not in pure liquids (10). The phenomenon manifests itself as dips or peaks in the T_1 or R_1 dispersion curve respectively and hence they are named quadrupole dips or peaks respectively. Early research on protein relaxation shows that the quadrupole dip behaviour varies slightly depending on the protein investigated and its properties (11).

At the moment the relaxation mechanisms are not completely understood and models proposed have evolved since the first theory (9). Sunde and Halle recently hypothesised that magnetisation is transferred to the amide ^{14}N through a three-step transfer from the bulk water via an intermediary proton (12).

Previous work predicted that the change in the modified proton relaxation rate due to nitrogen cross-relaxation depends linearly on the concentration of protein in the gel sample, according to the equation:

$$\Delta R_1 = R_1^{QD} - R_1^{0}$$

where ΔR_1 is the measured proton relaxation rate change due to cross-relaxation, R_1^{QD} is the relaxation rate at the observed quadrupolar frequency and R_1^{0} is the relaxation rate due to the lattice only (8).

In this study we chose to investigate a bio-medically relevant model system that would permit monitoring of the quadrupole dips via NMR relaxometry. The fibrin clot model system has been widely researched. Fibrin is the protein that forms the principal structural element of blood clots, which restrict blood loss while maintaining the circulation of blood (13). Figure 1 illustrates the conversion of fibrinogen (a soluble protein found in blood plasma) to polymerised fibrin and then to mechanically stable cross-linked fibrin (14). When a fibrin clot forms, other proteins become trapped in this network. As the most abundant protein in blood plasma, albumin is trapped in the clot and leads to a change in clot structure and characteristics (15).

NMR based techniques have been previously used to investigate various properties of thrombi, such as the effect on clot retraction on lysis using MRI (16), as well as the use of MRI contrast agents with high specificity for fibrin (17-20) or FXIII (21) in thrombus detection. The aim of this work was to expand on our preliminary work (4) on the measurement of quadrupole peaks in R_1 and to investigate the linearity between quadrupole peak amplitude and protein concentration in fibrin protein gels. We also investigated whether the quadrupole peak amplitude is dependent on fibrin cross-linking. As trapped proteins have an effect on the characteristics of the fibrin clot, we investigated their effect on the quadrupole peaks observed in fibrin gel in order to evaluate the robustness of this method for future *in vivo* detection. This was done through the addition of albumin, the most abundant protein in blood plasma.

Methods

Fibrin(ogen) Samples for NMR relaxometry Samples: The protocol for fibrin formation was based on established methods (22). Aqueous fibrinogen samples of 1.2 mL were prepared using human fibrinogen (Hyphen Biomed, France) at 10 different concentrations, ranging from 0.1 to 10 mg mL^{-1}, in 0.2 % (w/v) agarose (Sigma Aldrich, UK), 75 mM Tris buffer (pH 7.8), 22 mM NaCl and 5 mM $CaCl_2$. Fibrinogen was stored as 20 mg mL^{-1} frozen aliquots, defrosted at room temperature and placed on ice. Agarose was added to ensure sample homogeneity; it was dissolved in 75 mM Tris buffer (pH 7.8), 22 mM NaCl and 5 mM $CaCl_2$, boiled in a microwave oven for 30 s and allowed to cool to 44 °C before being added to fibrinogen and buffer. For clotted fibrin gel samples, clotting was rapidly induced by the addition of thrombin at 0.4 IU mL^{-1} (Sigma Aldrich, UK). Fully cross-linked fibrin samples were made using the same procedure but with the addition of 3.3 U mL^{-1} transglutaminase FXIII (Aventis, France) and 10 mg mL^{-1} fibrinogen. These were compared to fibrin clots prepared with 1 mM transglutaminase inhibitor 1,3-dimethyl-2-[(2-oxopropyl) thio]imidazolium chloride (23), which inhibits fibrin cross-linking. The inhibitor studies were undertaken because the human fibrinogen used was contaminated with FXIII (contamination was confirmed by sodium dodecyl sulfate polyacrylamide gel electrophoresis (SDS-PAGE) (data not shown) (24)). Human serum albumin was incorporated in some fibrin samples: 3 mg mL^{-1} fibrin(ogen) clot samples were prepared as above in the presence of 40 mg mL^{-1} human serum albumin (Sigma Aldrich, UK).

Aqueous fibrinogen and fibrin clot samples were prepared in small glass tubes for ease of preparation and the 1.2 mL preparations were immediately transferred to standard NMR sample tubes and incubated for 2 h before data acquisition. Clot turbidity in relation to clot formation was monitored by 405 nm visible light absorbance using a Multiskan Ascent (Thermo Labsystems, UK) plate reader. The reaction plateau was reached after approximately 1 h (data not shown). Sample preparation and incubation was done in a 37 °C water bath. Experimental procedures were repeated three times on different days.

NMR relaxometry measurement: Relaxation rate measurements were carried out using a fast field-cycling NMR relaxometer (SMARtracer, Stelar S.r.l, Italy). A temperature controller with ± 0.1 °C accuracy was used. The spin-lattice relaxation time T_1 was measured using an inversion recovery pulse sequence using 30 different evolution fields linearly selected between 1.5 and 3.5 MHz (proton Larmor frequency), in order to measure the two higher-frequency quadrupole dips. The polarisation time and field used were 5 s and 5 MHz respectively and the ramp time was set to 2.5 ms. The acquisition field was set to 7.2 MHz.

Data analysis: The values of T_1 were calculated using a monoexponential model, checking that the R^2 (25) values of the fits were greater than 0.999. The data was analysed by a curve fitting algorithm (Matlab) using a model derived from the literature (9) using Lorenzian bells for peaks R_1^{QD} and a power law for the background R_1^0 signal. It can be noted that the data from fibrinogen cannot be used as a background line since clotting affects the spin-lattice relaxation in the fibrin samples.

Results

Quadrupole peaks were observed in a sample of clotted 10 mg mL^{-1} fibrin. Figure 2 shows an experimental R_1-dispersion curve of a sample of 10 mg mL^{-1} fibrin, together with a fitted curve. The two higher-frequency quadrupole peaks are clearly observed over the baseline spanning the frequency range of 1.5 to 3.5 MHz. The figure also shows a dispersion curve obtained from fibrinogen alone, which exhibits no quadrupolar peaks, as expected from the mobile protein in solution.

The amplitude of the quadrupole peaks arising from varied concentrations of fibrin was examined. Fibrin clots were prepared from fibrinogen solutions whose concentration varied from 0.1 to 10 mg mL^{-1}. Measurements were made at 37 °C. Figure 3 shows R_1 as a function of the proton Larmor frequency for these samples in the range of 1.5 to 3.5 MHz. The progressive increase in amplitude of the quadrupole peaks can be seen as the fibrin concentration increases (from bottom to top dispersion curves respectively). Figure 4 shows the fitted quadrupolar peak amplitude as a function of fibrinogen concentration. A linear dependence is seen. Fibrinogen alone exhibited no quadrupole peaks at any of the concentrations (data not shown but illustrated in Fig 2 for the highest concentration).

The effect of temperature on quadrupole peak amplitude was investigated (Figure 5) by acquiring a proton R_1 dispersion curve for fibrin clot samples of varied concentrations measured at 25 and 37 ± 0.1 °C (after incubation at 37 °C for 2 h). The fitted ΔR_1 value of the 25 and 37 °C curves measured $(94.4 \pm 5) \times 10^{-3}\ s^{-1}$ and $(87.4 \pm 7) \times 10^{-3}\ s^{-1}$ respectively.

The effect of increasing fibrin clot rigidity was examined by inducing full cross-linking. Figure 6 illustrates that there was no effect on the proton R_1 dispersion curve upon addition of FXIII. The fibrinogen used was contaminated with FXIII and so we examined the effect of an inhibitor of transglutaminases, including FXIII (23), which again had no effect. When the curves were fitted (not shown), the R^2 value of the fits for fibrin, fibrin with added FXIII or

inhibitor were 0.99, 0.99 and 0.97 respectively. The fitted quadrupole peak amplitude ($\times 10^{-3}$ s^{-1}) of the various 10 mg mL^{-1} fibrin samples were 91 ± 8 for fibrin, 95 ± 12 for fibrin with added FXIII and 92 ± 3 for fibrin with added inhibitor (Table 1).

The effect of the addition of albumin on fibrin quadrupole peak amplitude was studied. The physiological concentration range of fibrinogen in blood plasma is 2 – 4.5 mg mL^{-1} and the concentration of albumin is 35 to 55 mg mL^{-1} (26). The amplitude of the 3 mg mL^{-1} fibrin clots with or without added albumin (40 mg mL^{-1}) measured at 37 °C were $(48.1 \pm 7) \times 10^{-3}$ s^{-1} and $(23.1 \pm 7) \times 10^{-3}$ s^{-1} respectively. No quadrupolar signal was observed from fibrinogen samples with added albumin (data not shown).

Discussion

It is evident that fibrin clots exhibit significant quadrupole peaks in their R_1 dispersion curves, as seen in Figures 2 and 3. The quadrupole peak is generated when the motion-restricted fibrin polymer is formed in a clot. Non-clotted fibrinogen samples did not present such features (Figure 2), indicating the specificity of this technique for immobilised proteins. Furthermore, the amplitude of the quadrupole peaks, ΔR_1, is linear with protein concentration in the source solution (Figure 4).

It should be noted that the curve fitting algorithm may introduce a bias at low concentrations of fibrin. Even when no clotting occurs, noise in the dispersion curve may be interpreted as a peak by the algorithm. This gives a residual apparent signal at fibrin concentrations lower than 1 mg mL^{-1} that depends on the standard deviation of the dispersion curve relative to the baseline. The signal-to-noise ratio measured from the averaged results indicates a detection threshold of 1.04 mg mL^{-1} starting fibrinogen concentration. This can be lowered by using averaging during the data acquisition, but it is still lower than the typical physiological concentration of fibrinogen in plasma (2 to 4.5 mg mL^{-1}) (26). The histogram of the residuals from the fits of the quadrupole peaks was close to a Gaussian distribution (data not shown), indicating randomly distributed noise, with a centre shifted by $(0.12 \pm 0.56) \times 10^{-3}$ s^{-1}. This indicates a negligible bias in the fit of the quadrupole peaks.

The effect of temperature on R_1 (Figure 5) was investigated and the slope of the mean peak amplitude analysed at 25 °C was $(9.0 \pm 0.6) \times 10^{-3}$ s^{-1}, whilst at 37 °C the mean amplitude was $(7.7 \pm 0.9) \times 10^{-3}$ s^{-1}. A p-value (25) of greater than 0.99 revealed a small but significant difference in the quadrupole peak amplitude between the results obtained at 25 °C and 37 °C.

Thermal energy increases the Brownian motion of the molecules as stated in the literature (19), therefore may affect the facilitated access of water molecules to the NH site.

We also investigated whether gel rigidity through fibrin cross-linking affected fibrin quadrupolar peak amplitude. This was done by clotting fibrinogen in the absence and presence of FXIII (Figure 6). Table 1 lists the measured ΔR_1 values for the different samples. A paired T-Test (25) was performed on the data. The p-values for (i) fibrin compared with cross-linked fibrin (+FXIII), and 9ii) fibrin compared with fibrin in which the action of FXIII was inhibited were 0.68 and 0.58 respectively, meaning that there is no significant difference between the amplitudes. This indicates there is no effect on fibrin peak amplitude from gel rigidity, within the range of these measurements. This suggests that the quadrupolar peak signal is not dependent on how immobilised the protein is but rather that once it is sufficiently immobilised the signal is generated and is not affected. This finding indicates that the quadrupole signal is generated when fibrin is formed, and may reflect polymerization, but this was not formally assessed.

Trapped proteins affect the structure and characteristics of the fibrin clot. An increase in the mean quadrupole peak amplitude of fibrin was observed with the addition of albumin (at physiological concentration). A quadrupole dip in T_1 in serum albumin has been documented previously in the literature (5). An explanation for this result may be that albumin is trapped in the fibrin clot gel and hence is sufficiently immobilised. This may have an effect on the residence time of albumin, therefore allowing magnetisation to be transferred to the amide ^{14}N from the bulk water as suggested by Sunde and Halle (12) and relaxation to occur. Further work will have to be done to investigate the dynamics and characteristics of albumin when trapped in the gel network that give it this property. Observations of samples in which albumin was added to 10 mg mL^{-1} fibrinogen (data not shown) gave no quadrupole peaks in the dispersion curve.

Conclusions

Quadrupole peaks in the R_1 dispersion plots of human fibrin have been demonstrated and linearity has been established over a range of concentrations that cover physiological concentration and temperature. This is in agreement with previous work on protein samples (12). An increase in clot rigidity and mechanical stability from the presence of fibrin cross-linking did not lead to a significant change in peak amplitude, indicating that ΔR_1 amplitude is

sensitive to fibrin formation but not to cross-linking in this particular system. The temperature at which an NMR measurement of a fibrin clot is taken does affect the quadrupolar peak amplitude. There is a significant effect on ΔR_1 amplitude with the addition of albumin to fibrin clots and further work needs to be done to investigate this effect.

Our results showed that cross-linking levels will not affect quadrupolar cross-relaxation in future *in vivo* studies but that proteins trapped in the clot such as albumin may significantly increase the amplitude of that signal. Potentially, future work will lead to a novel method using FFC-MRI to establish the concentration of *in vivo* fibrin. This may have a clinical role in the detection and treatment of thrombi formed when haemostasis is deregulated.

Acknowledgments

The authors acknowledge financial support for the FFC-MRI project from Research Councils UK and the Engineering and Physical Sciences Research Council, under the Basic Technology scheme (grant no EP/E036775/1). We would like to show our appreciation to Dr. G. Davies and Mrs. N. Moore for their assistance. We are also grateful to Prof. B. Halle and Dr E.P. Sunde (Lund University) for their help with the data analysis model.

References

1. Kimmich R, Anoardo E. Field-cycling NMR relaxometry. Progress in Nuclear Magnetic Resonance Spectroscopy 2004;44:257-320.

2. Hallenga K, Koenig SH. Protein rotational relaxation as studied by solvent ^{1}H and ^{2}H magnetic relaxation. Biochemistry 1976;15:4255-64.

3. Kimmich R. Field cycling in NMR relaxation spectroscopy: Applications in biological, chemical and polymer physics. Bull Magn Reson 1980;1:195-218.

4. Lurie DJ, Aime S, Baroni S, Booth NA, Broche LM, Choi C-, Davies GR, Ismail S, Ó hÓgáin D, Pine KJ. Fast field-cycling magnetic resonance imaging. Comptes Rendus Physique 2010;11:136-48.

5. Winter F, Kimmich R. NMR field-cycling relaxation spectroscopy of bovine serum albumin, muscle tissue, micrococcus luteus and yeast. $^{14}N^{1}H$-quadrupole dips. BBA - General Subjects 1982;719:292-8.

6. Blinc R, Mali M, Osredkar R, Prelesnik A, Seliger J, Zupančič I, Ehrenberg L. ^{14}N NQR spectroscopy of some amino acids and nucleic bases via double resonance in the laboratory frame. J Chem Phys 1972;57:5087-93.

7. Seliger J, Osredkar R, Mali M, Blinc R. ^{14}N quadrupole resonance of some liquid crystalline compounds in the solid. J Chem Phys 1976;65:2887-91.

8. Jiao X, Bryant RG. Noninvasive measurement of protein concentration. Magnetic Resonance in Medicine 1996;35:159-61.

9. Winter F, Kimmich R. Spin lattice relaxation of dipole nuclei (I = 1/2) coupled to quadrupole nuclei (S = 1). Mol Phys 1982;45:33-49.

10. Koenig SH. Theory of relaxation of mobile water protons induced by protein NH moieties, with application to rat heart muscle and calf lens homogenates. Biophys J 1988;53:91-6.

11. Koenig SH, Schillinger WE. Nuclear magnetic relaxation dispersion in protein solutions. I. apotransferrin. J Biol Chem 1969;244:3283-9.

12. Sunde EP, Halle B. Mechanism of ^{1}H-^{14}N cross-relaxation in immobilized proteins. Journal of Magnetic Resonance 2010;203:257-73.

13. Weisel JW. Fibrinogen and fibrin. Advances in Protein Chemistry 2005;70:247-99.

14. Ariëns RAS, Lai T-, Weisel JW, Greenberg CS, Grant PJ. Role of factor XIII in fibrin clot formation and effects of genetic polymorphisms. Blood 2002;100:743-54.

15. Wilf J, Gladner JA, Minton AP. Acceleration of fibrin gel formation by unrelated proteins. Thromb Res 1985;37:681-8.

16. Blinc A, Keber D, Lahajnar G, Zupancic I, Zorec-Karlovsek M, Demsar F. Magnetic resonance imaging of retracted and nonretracted blood clots during fibrinolysis in vitro. Haemostasis 1992;22:195-201.

17. Sirol M, Fuster V, Badimon JJ, Fallon JT, Moreno PR, Toussaint J-, Fayad ZA. Chronic thrombus detection with in vivo magnetic resonance imaging and a fibrin-targeted contrast agent. Circulation 2005;112:1594-600.

18. Overoye-Chan K, Koerner S, Looby RJ, Kolodziej AF, Zech SG, Deng Q, Chasse JM, McMurry TJ, Caravan P. EP-2104R: A fibrin-specific gadolinium-based MRI contrast agent for detection of thrombus. J Am Chem Soc 2008;130:6025-39.

19. Spuentrup E, Botnar RM, Wiethoff AJ, Ibrahim T, Kelle S, Katoh M, Özgun M, Nagel E, Vymazal J, Graham PB, Günther RW, Maintz D. MR imaging of thrombi using EP-2104R, a fibrin-specific contrast agent: Initial results in patients. Eur Radiol 2008;18:1995-2005.

20. Sirol M, Aguinaldo JGS, Graham PB, Weisskoff R, Lauffer R, Mizsei G, Chereshnev I, Fallon JT, Reis E, Fuster V, Toussaint J-, Fayad ZA. Fibrin-targeted contrast agent for improvement of in vivo acute thrombus detection with magnetic resonance imaging. Atherosclerosis 2005;182:79-85.

21. Tei L, Mazooz G, Shellef Y, Avni R, Vandoorne K, Barge A, Kalchenko V, Dewhirst MW, Chaabane L, Miragoli L, Longo D, Neeman M, Aime S. Novel MRI and fluorescent

probes responsive to the factor XIII transglutaminase activity. Contrast Media and Molecular Imaging 2010;5:213-22.

22. Mutch NJ, Robbie LA, Booth NA. Human thrombi contain an abundance of active thrombin. Thrombosis Haemostasis 2001;86:1028-34.

23. Mutch NJ, Koikkalainen JS, Fraser SR, Duthie KM, Griffin M, Mitchell J, Watson HG, Booth NA. Model thrombi formed under flow reveal the role of factor XIII-mediated cross-linking in resistance to fibrinolysis. Journal of Thrombosis and Haemostasis 2010;8:2017-24.

24. McKee PA, Rogers LA, Marler E, Hill RL. The subunit polypeptides of human fibrinogen. Arch Biochem Biophys 1966;116:271-9.

25. Montgomery DC. Design and Analysis of Experiments. John Wiley and Sons. 2005.

26. Putnam FW. Perspectives - Past, Present, and Future. In: Putnam FW (ed.). The Plasma Proteins: Structure, Function and Genetic Control. 2nd Edition, Vol. I. Academic Press; 1975.

Table 1

Average quadrupole peak amplitude (ΔR_1) of 10 mg mL^{-1} fibrin +/- FXIII or FXIII inhibitor

Sample	Fibrin	Fibrin + FXIII	Fibrin + FXIII Inhibitor
Amplitude ($\times 10^{-3}$ s^{-1})	91 ± 8	95 ± 12	92 ± 3
Paired T-test p-value (compared with Fibrin sample)	–	0.68	0.58

Figure 1

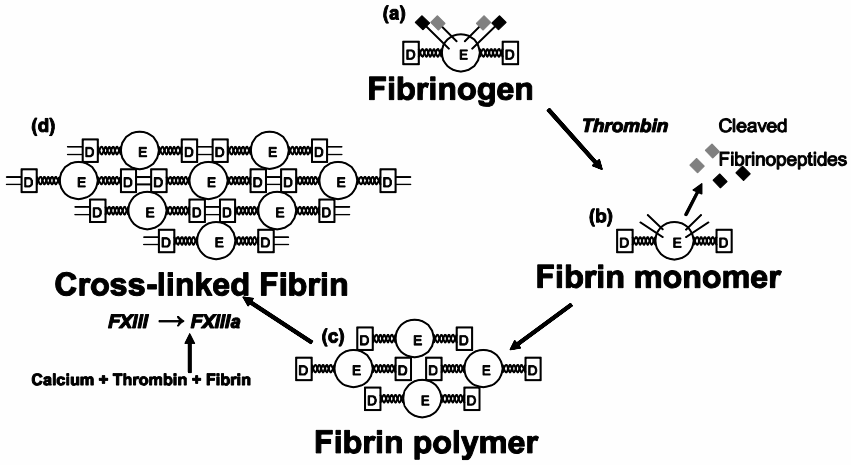

Figure 1: (a) Fibrinogen has a central E domain joined by segment coils to two D outer domains. (b) Thrombin cleavage releases firstly fibrinopeptide A and then fibrinopeptide B from the central E domain, exposing shielded fibrin polymerisation sites. A fibrin monomer is formed. (c) A fibrin clot is formed by fibrin polymerisation as the exposed sites on the E domain have strong affinity for the D domain of opposite monomers (13). (d) The activated transglutaminase factor XIIIa (FXIIIa) causes fibrin matrix maturation and stabilisation via covalently cross-linked flanking fibrin unit D domains (14).

Figure 2

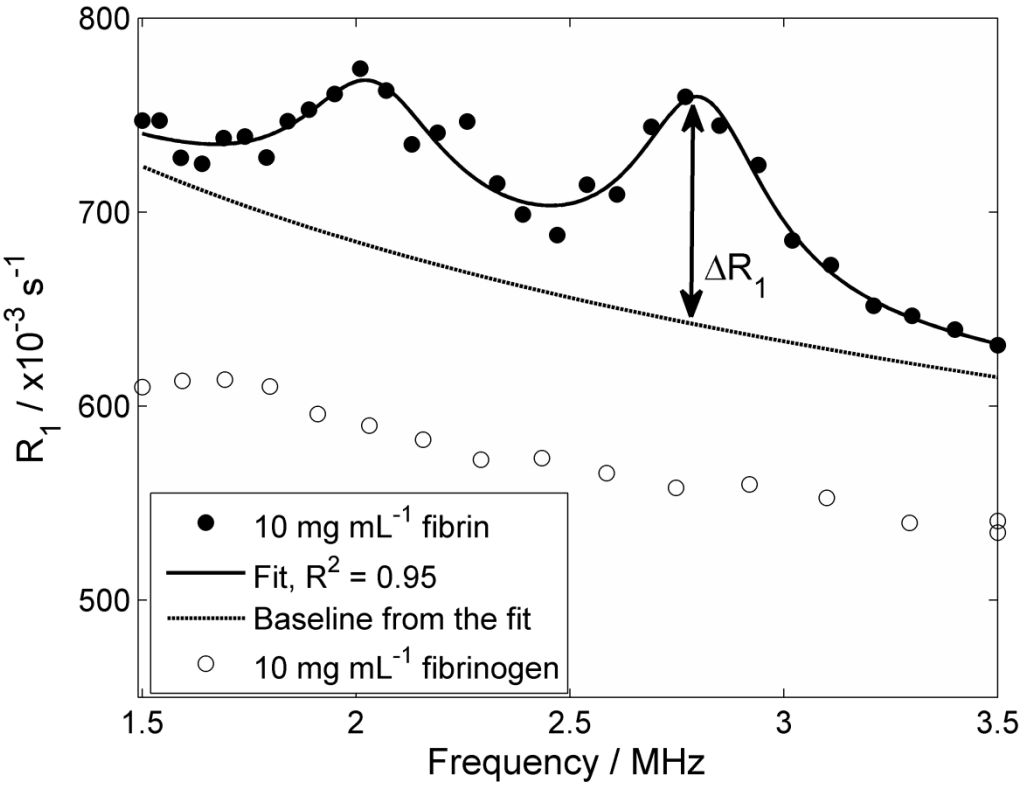

Figure 2: Proton R_1 dispersion measurements (filled circle) of a sample of 10 mg mL^{-1} fibrin in the region of the quadrupole peaks compared with fibrinogen (empty circle). The solid line shows the fitted curve based on the model (see text) and the baseline (dashed line) is a power law provided by the model used for curve fitting. ΔR_1 (8) (solid double ended arrow) is the measured quadrupole peak amplitude. Unfilled circles show proton R_1 dispersion measurements from a sample of 10 mg mL^{-1} fibrinogen, demonstrating the lack of quadrupole peaks from the solution of mobile protein.

Figure 3

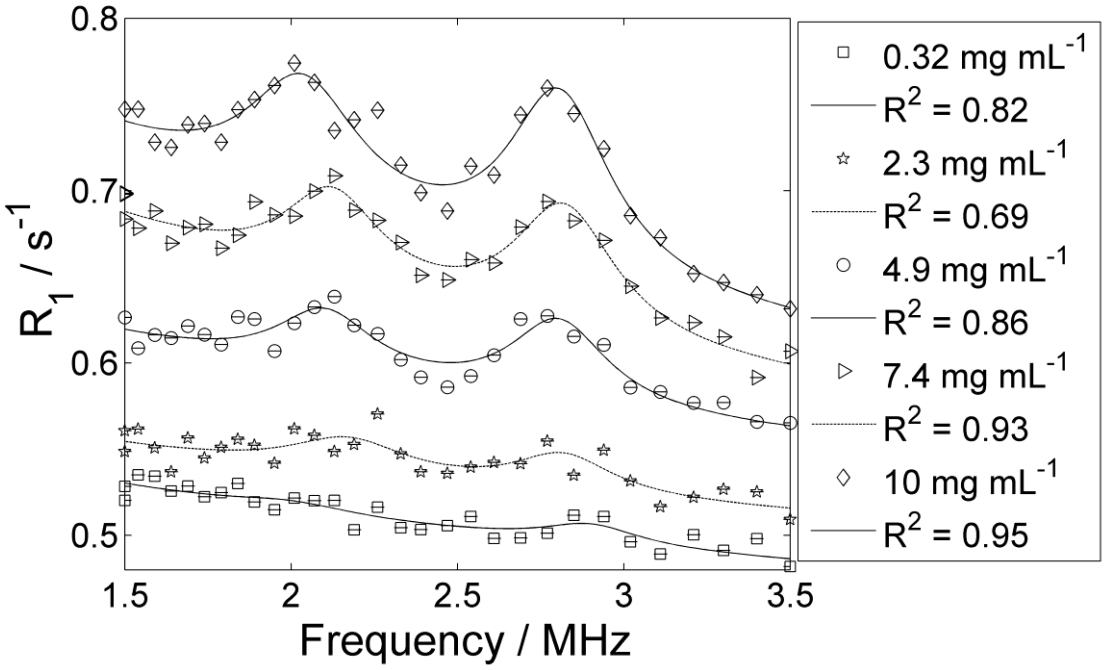

Figure 3: Data obtained showing the variation of the proton spin-lattice relaxation rate R_1 with proton Larmor frequency (MHz) from samples of varying starting concentrations of fibrinogen. Dispersion plots were fitted as described in the text. The curves from bottom to top correspond to increasing concentrations of fibrin, from 0.1 to 10 mg mL^{-1} measured at 37 °C.

Figure 4

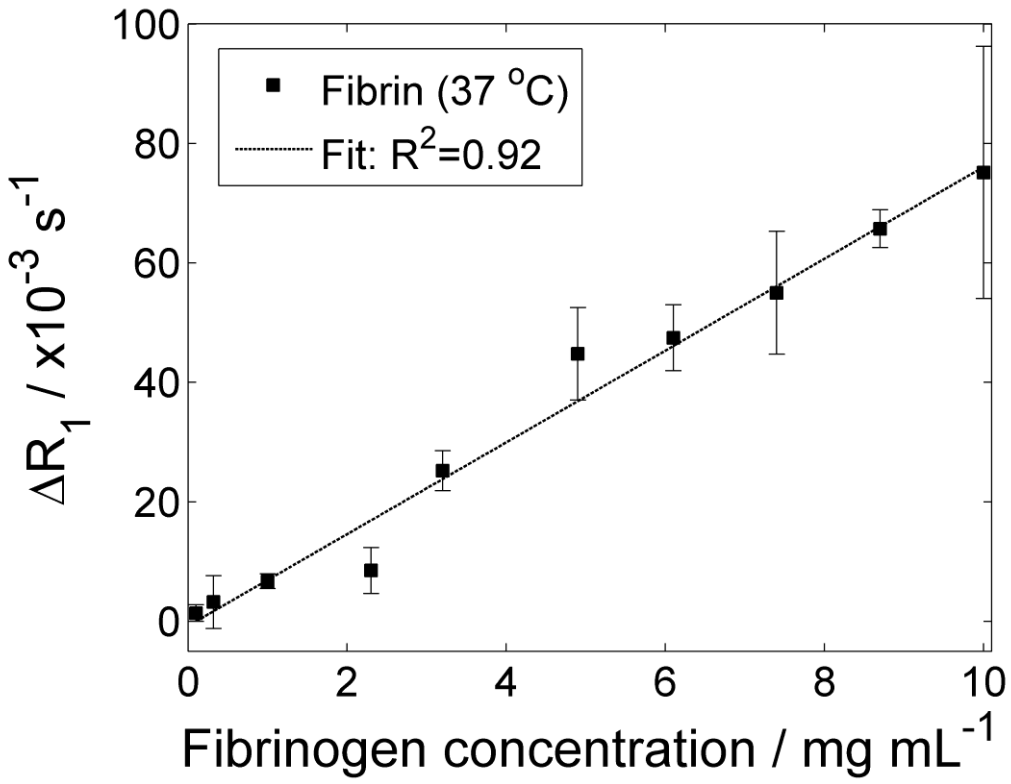

Figure 4: Average quadrupole peak amplitude as a function of fibrinogen concentration.

Figure 5

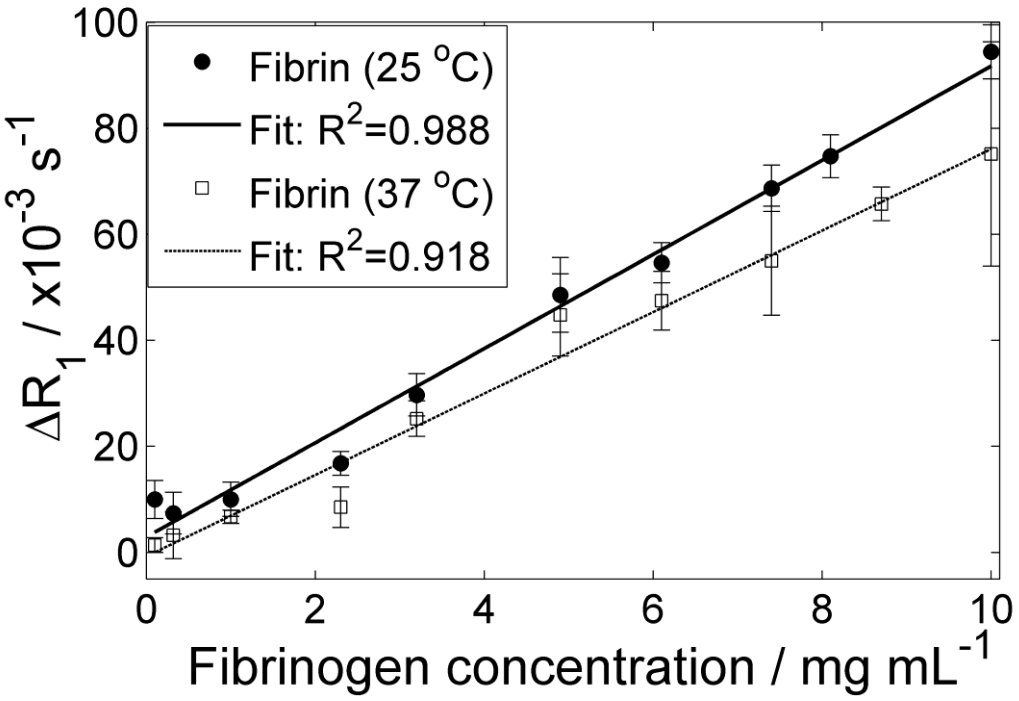

Figure 5: Quadrupole peak amplitude as a function of fibrinogen concentration, showing the effect on the slope of measuring at 25°C sample temperature (filled circle) and 37 °C (square).

Figure 6

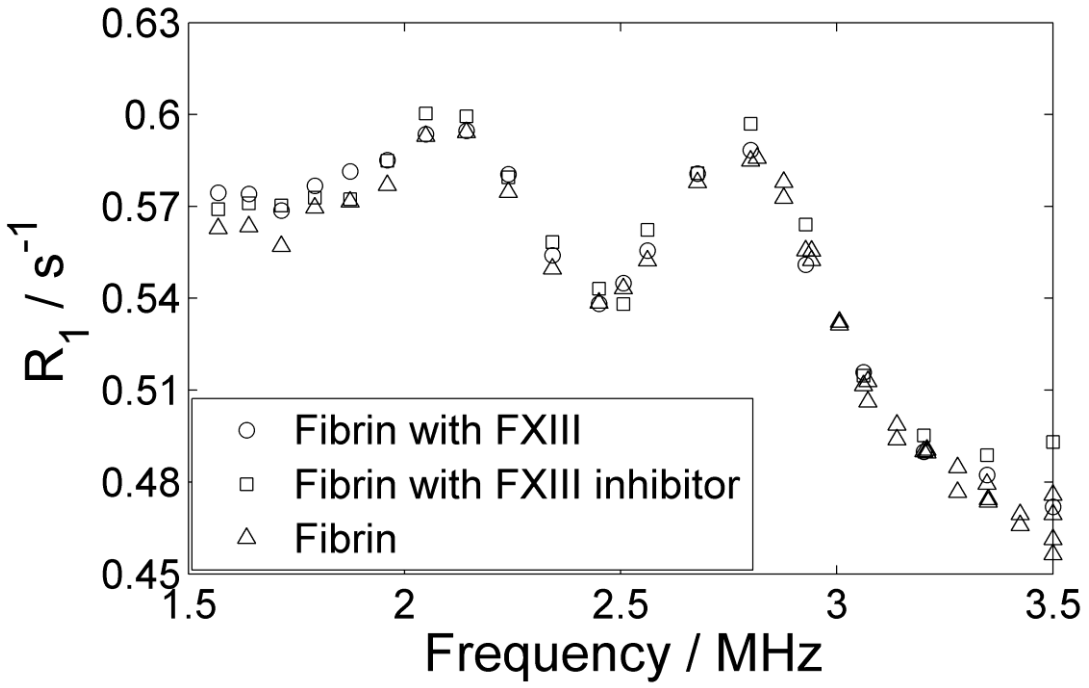

Figure 6: Effect on quadrupole peak amplitude of the addition of FXIII or FXIII inhibitor to 10 mg mL^{-1} fibrin clots measured at 37 °C.